C. R. Palevol 17 (2018) 143–151

Contents lists available at ScienceDirect

Comptes Rendus Palevol

www.sciencedirect.com

Human Palaeontology and Prehistory

Preliminary dating of the Mansu-Ri and Wondang-Jangnamgyo Early Paleolithic sites

Datations préliminaires des sites du Paléolithique ancien de Mansu-Ri et Wondang-Jangnamgyo

Anne-Elisabeth Lebatard[a,*], Didier L. Bourlès[a], Samir Khatib[b], Thibaud Saos[c], Pierre Rochette[a], Régis Braucher[a], Kidong Bae[d]

[a] *Aix-Marseille Université, CNRS-IRD UM34 CEREGE, Technopôle de l'environnement Arbois-Méditerranée, BP 80, 13545 Aix-en-Provence cedex 4, France*
[b] *Laboratoire de préhistoire Nice Côte d'Azur, 15, boulevard Maurice-Maeterlinck, 06300 Nice, France*
[c] *Université de Perpignan Via Domitia, UMR-CNRS 7194, EPCC Centre européen de recherches préhistoriques, avenue Léon-Grégory, 66720 Tautavel, France*
[d] *Institute of Cultural Properties, Hanyang University, Sa 1-dong, Ansan-si, 425-791, Gyeonggi-do, South Korea*

ARTICLE INFO

Article history:
Received 14 September 2015
Accepted after revision 18 April 2016
Available online 11 June 2016

Handled by Amélie Vialet

Keywords:
Early Paleolithic
South Korea
Cosmogenic nuclides
Burial ages

Mots clés :
Paléolithique ancien
Corée du Sud
Nucléides cosmogéniques
Durées d'enfouissement

ABSTRACT

The lack of carbonates and fossils in Early Paleolithic open air river terrace sites in Korea makes chronological assessment difficult. Nevertheless, a paleomagnetic study of the thickest section (about 9 m) at Mansu-Ri (Locality IV) revealed only normal polarity, indicating an age younger than 0.78 Ma all along the section. In Mansu-Ri (Loc. IV), measurements of the in situ-produced ^{10}Be and ^{26}Al concentrations in two pebbles yield similar ^{26}Al/^{10}Be burial durations ranging from a minimum duration of 225 ka to a maximum duration of 621 ka. In Wondang-Jangnamgyo, two pebbles yield different ^{26}Al/^{10}Be burial durations with a minimum duration of 235 ka and a maximum duration of 495 ka for one and ranging from 975 ka to 3.2 Ma for the other. This last unrealistically old burial duration range most likely results from a complex history of successive burials and expositions. Interestingly, by analogy with the Chinese loess section, the obtained minimum burial durations are coherent with the paleomagnetism result interpretation associating to glacial cycles the 3 paleosoils covering the samples dated at Mansu-Ri.

RÉSUMÉ

La médiocre préservation des carbonates et des fossiles dans les terrasses alluviales aériennes des sites coréens du Paléolithique ancien complique leur cadrage chronologique. Une étude paléomagnétique de la section la plus épaisse (environ 9 m) du site de Mansu-Ri (localité IV) a néanmoins mis en évidence une polarité normale, suggérant pour l'ensemble de la section un âge inférieur à 0,78 Ma. Pour ce site, la mesure des concentrations en ^{10}Be et ^{26}Al produits in situ dans deux galets de quartz conduisent à des durées ^{26}Al/^{10}Be

* Corresponding author.
E-mail addresses: lebatard@cerege.fr (A.-E. Lebatard), bourles@cerege.fr (D.L. Bourlès), samirkhatib@aol.com (S. Khatib), saos@cerptautavel.com (T. Saos), rochette@cerege.fr (P. Rochette), braucher@cerege.fr (R. Braucher), bkd5374@gmail.com (K. Bae).

https://doi.org/10.1016/j.crpv.2016.04.008

d'enfouissement similaires, comprises entre une durée minimum de 225 ka et une durée maximum de 621 ka. Pour Wondang-Jangnamgyo, les deux galets sélectionnés conduisent à des durées $^{26}Al/^{10}Be$ d'enfouissement différentes, comprises entre une durée minimum de 235 ka et une durée maximum de 495 ka pour l'un, et entre 975 ka et 3,2 Ma pour l'autre. Ces dernières durées d'enfouissement minimales et maximales résultent fort probablement d'une histoire complexe d'enfouissements et d'expositions successifs du galet étudié. Les durées minimales d'enfouissement obtenues sont cohérentes avec l'interprétation des résultats issus de l'étude du paléomagnétisme qui, par analogie avec la section de lœss chinois, associe à des cycles glaciaires les 3 paléosols recouvrant les échantillons datés à Mansu-Ri.

1. Introduction

The advent of the Accelerator Mass Spectrometry (AMS) technique has offered opportunities to develop several dating methods linked to the detection and measurements of cosmogenic nuclide concentrations such as carbon 14, beryllium 10 and aluminum 26 (^{14}C, ^{10}Be, ^{26}Al; e.g., Bourlès, 1992; Granger, 2006). One of these new dating methods, developed less than fifteen years ago, is based on the temporal exponential decrease of the $^{26}Al/^{10}Be$ ratio in substrates containing siliceous minerals that have been exposed to the cosmic ray before being buried under deposits that protect them from secondary cosmic ray radiation (e.g., Granger and Muzikar, 2001).

This burial duration dating method initially used to date quartz gravels in caves in order to establish river incision rates (Granger and Muzikar, 2001) was then applied successfully to several sites of paleontological and archaeological interest. Indeed, this method made it possible to date the Hominin sites from the cave of Sterkfontein in South Africa, recently re-evaluated at ~ 3.7 Ma (Granger et al., 2015), then that of Sima del Elefante in Atapuerca (Spain) at ~1.1 Ma (Carbonell et al., 2008). More recently, it was applied to an Early Acheulean site, near the town of Windsorton in South Africa, to determine the age of the Rietputs Formation, estimated between 1.2 and 1.7 Ma (Gibbon et al., 2009), and to the site of Zhoukoudian in China. In this last case, it involved a question of the age of *Homo erectus*, named "man of Beijing", which now is estimated at ~0.8 Ma (Guanjun Shen et al., 2009). Also in Asia, the $^{26}Al/^{10}Be$ dating method applied to 6 quartz artefacts collected in the Paleolithic site of Attirampakkam postponed the arrival of the first hominins on the Indian peninsula at 1.51 Ma ± 0.09 Ma (Pappu et al., 2011). Lastly, the age of the *Homo erectus* of Kocabaş was re-evaluated as between 1.2 and 1.6 Ma (Lebatard et al., 2014a, 2014b).

Recent discoveries of more than a hundred ancient Paleolithic sites in South Korea with which a rich lithic industry is associated (de Lumley et al., 2011) updated hominin dispersion in the Asiatic East and the settlement history of the Korean peninsula. In these sites, mainly in open-air fluviatile context, rich industries were unearthed in siliceous detrital sediments where no fauna was conserved. Only a few cave sites have yielded large mammal faunas in association with Early Paleolithic industries, reflecting the great antiquity of the hominin presence in the Korean peninsula. In the absence of faunas, their chronological frameworks are less certain. To obtain radiometric dates, several dating methods (OSL, ESR, IRSL...) were employed at some sites, but the first attempts were inconclusive or inconsistent (de Lumley et al., 2011 and references therein) and the ancient Paleolithic sites remain poorly dated in Korea.

Among these open-air Early Paleolithic sites, the Mansu-Ri (Figs. 1 and 2) and Wondang-Jangnamgyo (Figs. 1 and 3) areas appear suitable to attempt absolute dating. Here, we present the preliminary results obtained using the burial dating method to determine the burial duration of quartz pebbles from these two South Korean Early Paleolithic sites. At Mansu-Ri (Locality IV) site, the thickness of the section allows to perform a paleomagnetic study whose data are compared to the determined burial durations obtained from the same site.

2. General Context

The two selected Paleolithic sites are open-air sites close to rivers. On both sites, lithic industries were mainly unearthed from soil horizons interbedded with sandy-clayey silt levels corresponding to flood, Aeolian and colluvium deposits (de Lumley et al., 2011).

The Mansu-Ri (Loc. IV) site, located in Cheongwon, Chungcheongbuk-do province, 108 km SSE from Seoul (36°37' N, 127°19' E; altitude: 27–45 m; Fig. 1), was excavated in 2006. Along the ~9 m deep excavated clay-sand sequence (Fig. 2), 5 archaeological levels contained nearly 400 lithic artifacts. Within the first meter, 3 tephras were identified whose oldest age is 90–95 ka (de Lumley et al., 2011, and references therein). The 5-c cultural layer at 6 m depth, from which 46 lithic tools typical from the ancient Paleolithic were unearthed, is the second richest layer. Two quartz pebbles from it were selected for burial dating (Fig. 4). The amplitude of the Mansu-Ri (Loc. IV) sedimentary sequence (up to 9 m) allows us to study the paleomagnetism along the longest section.

The Wondang-Jangnamgyo site, located in the Yeoncheon commune in the Gyeonggi-do province, 50 km north from Seoul (37°97'N, 126°89'E; altitude: 19–25 m, Fig. 1), was discovered in 2008. The longest 5 m section is composed by a succession of brownish clay levels covering pebbled sand with basalt blocs and basalt. However, dated

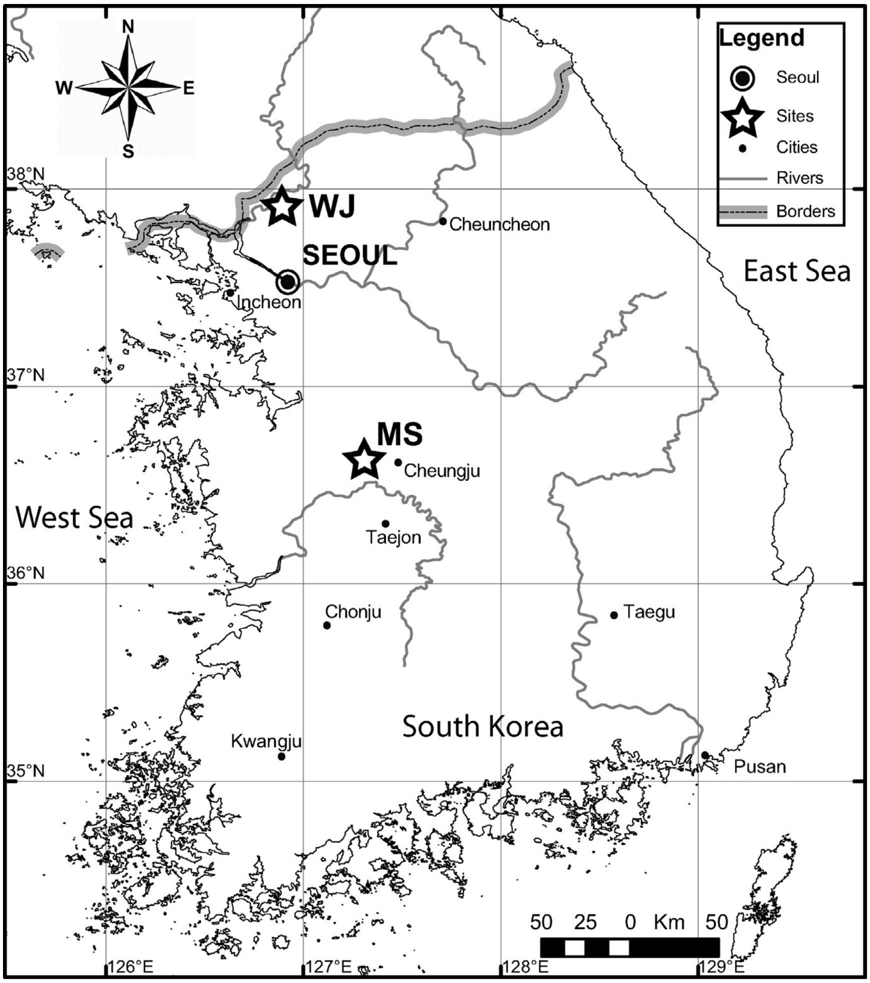

Fig. 1. Location of the Mansu-Ri (MS) and Wondang-Jangnamgyo (WJ) early Paleolithic sites in South Korea.

Fig. 1. Localisation des sites du Paléolithique ancien de Mansu-Ri (MS) et Wondang-Jangnamgyo (WJ) en Corée du Sud.

between 130 and 500 ka, the basalt has not yet allowed accurate absolute dating (de Lumley et al., 2011). Three archaeological levels were recognized within the mainly brownish clayed 2 first meters (Fig. 3). One of the two quartz pebbles (Fig. 4) selected for burial dating was sampled in the second archaeological level V (WJ S-3) and the second one in the second VII' layer (WJ S-1). Due to their repartitions in the excavation area, both were collected at 2 m depth (Fig. 3).

3. Materials and methods

3.1. Burial dating method

The burial dating method is based on the relative radioactive decay of two cosmogenic nuclides, ^{26}Al and ^{10}Be, which accumulate with a known ^{26}Al/^{10}Be production ratio of 6.61 within the quartz (SiO_2) mineral fraction (in situ production) of rocks exposed at the earth's crust surface due to nuclear reactions induced by the cosmic ray derived energetic particles on silicon (Si) and oxygen (O). Since the cosmic ray flux is efficiently attenuated by matter, the deposition of a few meters of sediments over a previously exposed surface (burial) leads to a sufficient reduction of the effective energetic particle flux to stop the ^{26}Al and ^{10}Be production. In the absence of production, the initial concentrations of each cosmogenic nuclide consequently start to radioactively decay according to their respective half-life, that is 0.717 ± 0.017 Ma for ^{26}Al (Granger, 2006; Samworth et al., 1972) and 1.387 ± 0.012 Ma for ^{10}Be (Chmeleff et al., 2010; Korschinek et al., 2010). The ^{26}Al concentration thus decreases approximately twice as fast as that of ^{10}Be, the ^{26}Al/^{10}Be ratio decreases exponentially with an apparent half-life of 1.48 ± 0.04 Ma. This method thus allows determining quartz mineral burial duration from 100 ka (100,000 years) to approximately 5 Ma (Granger and Muzikar, 2001).

The physico-chemical treatments performed on the four studied quartz pebbles as well as the accelerator mass spectrometry measurements at ASTER of their ^{10}Be and ^{26}Al concentrations followed the protocols and parameters fully described in Lebatard et al. (2014a) and references therein.

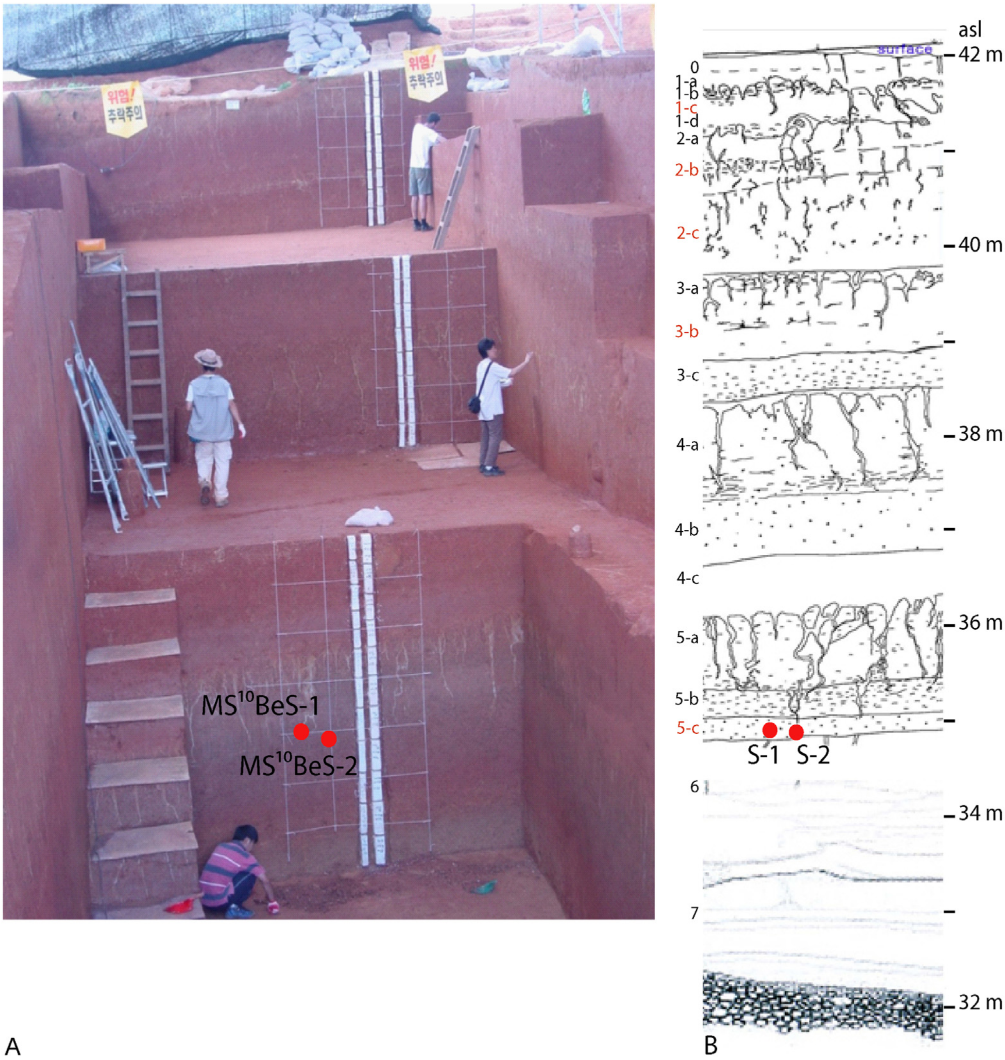

Fig. 2. Mansu-Ri Paleolithic site (Locality IV). A. Photo. The left plastered cores correspond to the paleomagnetic sampling. The two samples, $MS^{10}BeS$-1 and $MS^{10}BeS$-2, were collected 6 m beneath the surface (red points on the photo) in the fifth archaeological layer (Photo©S. Khatib). B. Synthetic stratigraphical log. The archaeological levels are indicated in red. The two samples, $MS^{10}BeS$-1 (S-1) and $MS^{10}BeS$-2 (S-2) came from the 5-c archaeological level (modified from de Lumley et al., 2011).

Fig. 2. Le site paléolithique de Mansu-Ri (localité IV). A. Photo. Les carottes plâtrées de gauche correspondent aux prélèvements pour l'étude paléomagnétique. Les deux échantillons, $MS^{10}BeS$-1 et $MS^{10}BeS$-2, ont été collectés à 6 m sous la surface (points rouges sur la photo) dans la cinquième couche archéologique (Photo©S. Khatib). B. Log stratigraphique synthétique. Les niveaux archéologiques sont indiqués en rouge. Les deux échantillons, $MS^{10}BeS$-1 (S1) et $MS^{10}BeS$-2 (S2), proviennent du niveau archéologique 5-c (modifié d'après de Lumley et al., 2011).

The concentrations measured for these two cosmogenic nuclides in the same quartz sample insure that they both record the same history in term of exposition, denudation and burial. They allow calculating the $^{26}Al/^{10}Be$ ratio associated to each sample and, consequently, to determine their corresponding burial duration and denudation rate using the method fully described in the SOM of Pappu et al. (2011).This modeling method is based on the equation (1) describing the evolution of the in situ produced cosmogenic nuclide concentration $C(x,\varepsilon,t)$ as a function of the depth (x), the denudation rate (ε) and the time (t):

$$C(x,\varepsilon,t) = C(x,0)\cdot e^{-\lambda t} + \frac{P_n \cdot e^{\frac{-x}{\Lambda_n}} \cdot \left(1 - e^{-(\lambda + \frac{\varepsilon}{\Lambda_n})t}\right)}{\frac{\varepsilon}{\Lambda_n} + \lambda} + \frac{P_{\mu sl} \cdot e^{\frac{-x}{\Lambda_{\mu sl}}} \cdot \left(1 - e^{-(\lambda + \frac{\varepsilon}{\Lambda_{\mu sl}})t}\right)}{\frac{\varepsilon}{\Lambda_{\mu sl}} + \lambda} + \frac{P_{\mu ft} \cdot e^{\frac{-x}{\Lambda_{\mu ft}}} \cdot \left(1 - e^{-(\lambda + \frac{\varepsilon}{\Lambda_{\mu ft}})t}\right)}{\frac{\varepsilon}{\Lambda_{\mu ft}} + \lambda} \quad (1)$$

where λ is the radioactive decay constant, P_n is the spallogenic production rate linked to the neutrons, $P_{\mu sl}$ and $P_{\mu ft}$ are production rates linked to slow and fast muons, respectively (Braucher et al., 2011 and associated references), Λ_n, is the neutrons attenuation length, and $\Lambda_{\mu sl}$ and $\Lambda_{\mu ft}$, are the slow and fast muons attenuation lengths, respectively. Modeling were computed using the parameters discussed in Braucher et al. (2011), including the $^{26}Al/^{10}Be$ spallogenic production rate ratio of 6.61 ± 0.50. Neutronic production rates have been scaled using (Stone, 2000) and are based on a weighted mean ^{10}Be spallation

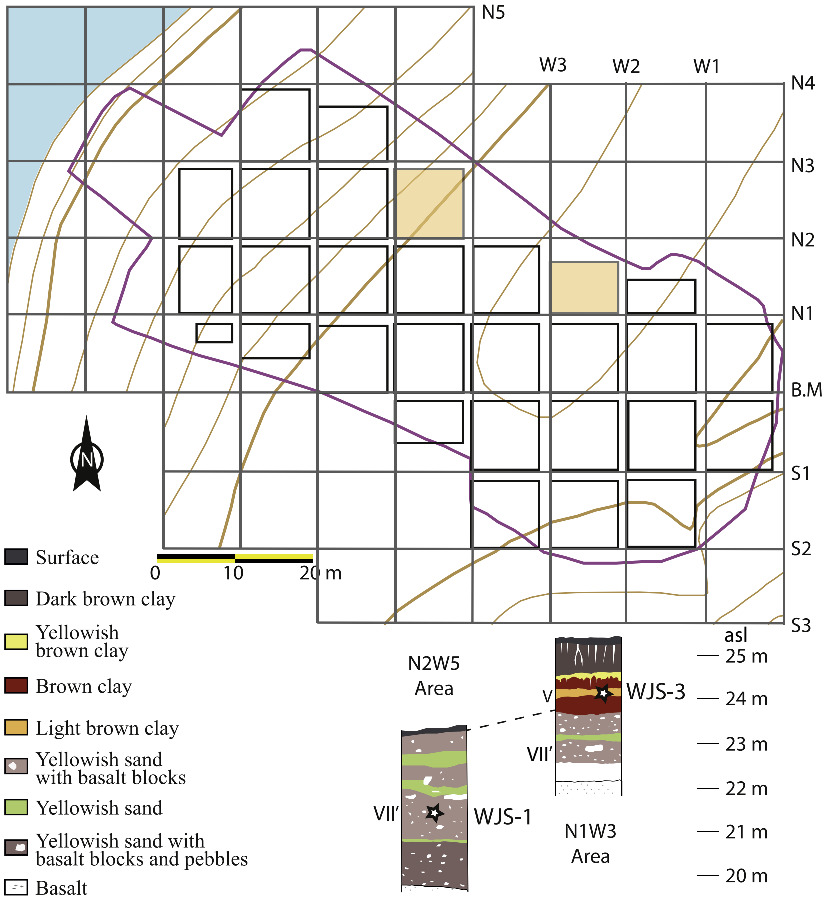

Fig. 3. The Wondang-Jangnamgyo paleolithic site. Map and stratigraphical logs of the site. The sampling location of WJ^{10}BeS-1 (WJS-1) and WJ^{10}BeS-3 (WJS-3) are reported on both map (yellow squares) and logs (stars) (modified from de Lumley et al., 2011).

Fig. 3. Le site paléolithique de Wondang-Jangnamgyo. Plan et logs stratigraphiques. La localisation d'échantillonnage de WJ^{10}BeS-1 (WJS-1) et WJ^{10}BeS-3 (WJS-3) est reportée sur le plan (carrés jaunes) et sur les logs (étoiles) (modifié d'après de Lumley et al., 2011).

production rate at sea level and high latitude (SLHL) of 4.03 ± 0.18 at g^{-1} a^{-1} (Molliex et al., 2013).

Uncertainties associated with the ratios, the durations and the denudation rates, reported as 1σ, result from the propagation of the uncertainties previously referred and described (Table 1).

The performed modeling method allows to determine minimum burial durations, based on the sole differential cosmogenic nuclides radioactive decay, and the estimated associated denudation rates (Table 1: "Model without post-burial production"), and maximized burial durations, based on the assumption that the environmental conditions remained relatively stable since the burial, and the associated denudation rates (Table 1: "Model with post-burial production"). Minimum burial durations are also obtained using the exposure–burial diagram (Fig. 5; e.g.,

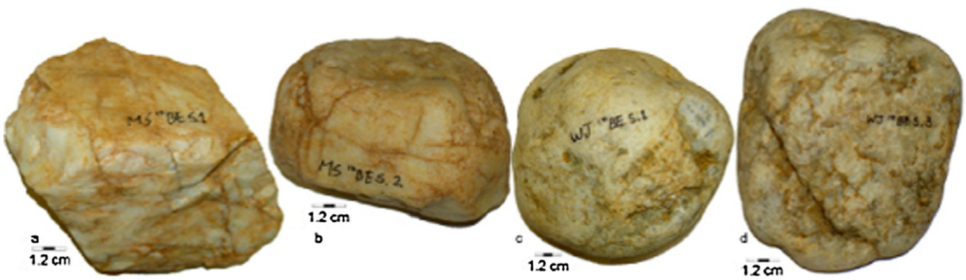

Fig. 4. The four quartz pebbles dated in this study. MS^{10}BeS-1 (a) and MS^{10}BeS-2 (b) were sampled at the Mansu-Ri site (Loc. IV); WJ^{10}BeS-1 (c) and WJ^{10}BeS-3 (d) at the Wondang-Jangnamgyo site.

Fig. 4. Les quatre galets de quartz datés dans cette étude. MS^{10}BeS-1 (a) et MS^{10}BeS-2 (b) ont été échantillonnés sur le site de Mansu-Ri (Loc. IV); WJ^{10}BeS-1 (c) et WJ^{10}BeS-3 (d) sur celui de Wondang-Jangnamgyo.

Table 1
In situ produced ^{26}Al and ^{10}Be concentrations, burial durations and denudations rates. Uncertainties (± 1σ) include only analytical uncertainties. The burial durations are in ka (1000 a). The denudation rates are given in m Ma^{-1} (meter per million years). The scaled neutronic production for the studied sites is 6.93 at g^{-1} a^{-1} for ^{10}Be and 45.83 at g^{-1} a^{-1} for ^{26}Al, slow muons production is 0.02 at g^{-1} a^{-1} for ^{10}Be and 1.12 at.g^{-1}.a^{-1} for ^{26}Al, and fast muons production is 0.05 at g^{-1} a^{-1} for ^{10}Be and 0.09 at g^{-1} a^{-1} for ^{26}Al (Braucher et al., 2011; Stone, 2000). Density is considered to be 2.2 g cm^{-3}. The chemical blank ratio are $2.84.10^{-15}$ and $1.84.10^{-15}$ for $^{10}Be/^{9}Be$ and $^{26}Al/^{27}Al$ ratio, respectively. The measured ratios are corrected from these values. W. dis. Qz: Weight of dissolved quartz; Gr.: graphically deduced from the exposure–burial diagram (Fig. 5). The graphically determined minimum burial durations were obtained considering the radioactive decay duration necessary to straightforwardly reach from the lower "steady erosion" curve of the "steady-state erosion island" the minimum $^{26}Al/^{10}Be$ ratio value considering the associated uncertainties. According to Pappu et al., 2011, the "Model without post-burial production" assuming that no cosmogenic nuclides were accumulated in the samples while buried (infinite burial depth) yields minimum burial duration. The "Model with post-burial production" assuming for modeling that the samples remained buried at their sampling depths and accumulated cosmogenic nuclides produced by muons yields maximized burial durations in a steady denudation over the burial period.

Tableau 1
Concentrations en ^{26}Al et ^{10}Be produits in situ, durées d'enfouissement et taux de dénudation. Les incertitudes (± 1σ) incluent seulement les incertitudes analytiques. Les durées d'enfouissement sont exprimées en ka (1000 a). Les taux de dénudation sont donnés en m Ma^{-1} (mètre par million d'années). La production neutronique établie pour les sites est 6,93 at g^{-1} a^{-1} pour le ^{10}Be et 45,83 at g^{-1} a^{-1} pour l'^{26}Al, la production par les muons lents est 0,02 at g^{-1} a^{-1} pour le ^{10}Be et 1,12 at.g^{-1}.a^{-1} pour l'^{26}Al, la production par les muons rapides est 0,05 at g^{-1} a^{-1} pour le ^{10}Be et 0,09 at g^{-1} a^{-1} pour l'^{26}Al (Braucher et al., 2011 ; Stone, 2000). La densité est 2,2 g cm^{-3}. Les rapports des blancs chimiques sont $2{,}84.10^{-15}$ et $1{,}84.10^{-15}$ pour les rapports $^{10}Be/^{9}Be$ et $^{26}Al/^{27}Al$, respectivement. Les rapports mesurés sont corrigés de ces valeurs. W. dis. Qz : poids de quartz dissous ; Gr. : graphiquement déduit du diagramme exposition–enfouissement (Fig. 5). Les durées d'enfouissement minimums déterminées graphiquement ont été obtenues en considérant la durée de décroissance radioactive nécessaire pour atteindre directement à partir de la courbe inférieure « érosion régulière » de « l'îlot des états stationnaires » la valeur du rapport $^{26}Al/^{10}Be$ minimum, compte tenu des incertitudes associées. Selon Pappu et al., 2011, le « Modèle sans production post-enfouissement », en supposant qu'aucun nucléide cosmogénique n'a été accumulé dans les échantillons au cours de l'enfouissement (profondeur d'enfouissement infinie) donne la durée d'enfouissement minimum. Le « modèle de production post-enfouissement », en supposant pour la modélisation que les échantillons soient restés enfouis à leurs profondeurs d'échantillonnage et accumulent des nucléides cosmogéniques produits par les muons, conduit à maximiser les durées d'enfouissement avec une dénudation stable au cours de la période d'enfouissement.

		Samples			
		MS^{10}BeS-1	MS^{10}BeS-2	WJ^{10}BeS-1	WJ^{10}BeS-3
	Depth (g.cm^{-2})	1320	1320	440	440
	W. dis. Qz (g)	29.0	28.7	29.4	29.5
	^{26}Al (10^5 at.g^{-1})	19.42 ± 0.88	24.59 ± 0.880	13.25 ± 1.87	9.23 ± 0.34
	^{10}Be (10^5 at.g^{-1})	3.50 ± 0.14	4.36 ± 0.15	3.75 ± 0.14	1.56 ± 0.05
	$^{26}Al/^{10}Be$	5.54 ± 0.33	5.64 ± 0.27	3.54 ± 0.52	5.91 ± 5.91
Model without post-burial production	Burial duration (ka)	396.7 ± 25.98	333.24 ± 18.09	1278.04 ± 188.97	331.91 ± 18.00
	Denudation before burial (m.Ma^{-1})	7.0 ± 0.4	5.6 ± 0.3	3.9 ± 0.6	17.8 ± 0.9
Model with post-burial production	Burial duration (ka)	464.23 ± 30.40	382.37 ± 20.76	2768.49 ± 409.34	589.28 ± 31.96
	Denudation before and after burial (m.Ma^{-1})	7.0 ± 0.4	5.7 ± 0.3	2.5 ± 0.4	18.8 ± 0.9
	Post-burial ^{26}Al produced (10^3 at.g^{-1})	129.15	117.36	888.11	238.20
	% post-burial prod /measured ^{26}Al	7	5	67	26
	Post-burial ^{10}Be produced (10^3 at.g^{-1})	12.90	11.22	116.89	25.68
	% post-burial prod /measured ^{10}Be	4	3	31	16
Exposure–Burial Diagram	Gr. min. burial duration (ka)	390 ± 125	330 ± 95	1275 ± 300	325 ± 100
	Gr. denudation before burial (m.Ma^{-1})	7.1 ± 0.3	5.7 ± 0.2	4.0 ± 0.2	17.7 ± 0.5

Granger, 2006), which aims to reproduce the minimum burial duration required to lead by radioactive decay from an initial $^{26}Al/^{10}Be$ concentration ratio conditioned by the denudation rate before burial to the measured ratio. The measured value may, however, also result from different and more complicated scenarios involving repeated burials and exposures which would obviously lead to significantly longer burial duration.

Table 1 summarizes all burial durations, denudation rates and post-burial concentrations calculated or graphically determined. The results are also plotted in the graph $^{26}Al/^{10}Be$ versus ^{10}Be (Fig. 5), also called "exposure–burial diagram" (e.g., Granger, 2006).

3.2. Paleomagnetism

Paleomagnetic sampling was performed all along the thickest sedimentary deposit section at Mansu-Ri (Locality IV; Fig. 2). All the sampling was handmade, oriented with a compass and consolidated with plaster tape. In these thus obtained 20–25 cm long and 7 cm large and wide oriented cores, cubes (7–8/core) were cut for natural remanent magnetization (NRM) measurements. The measurements were made using a 2G DC-Squid Superconducting Rock Magnetometer (SRM) at CEREGE. The direction of the characteristic remnant magnetization (ChRM) was retrieved by means of stepwise demagnetization using alternating field (AF) up to 60 or 80 mT.

4. Preliminary results

4.1. Burial dating

The results obtained for the two quartz pebbles from Mansu-Ri (Loc. IV; a and b, Fig. 4) sampled 6 m beneath the surface and for the two quartz pebbles from Wondang-

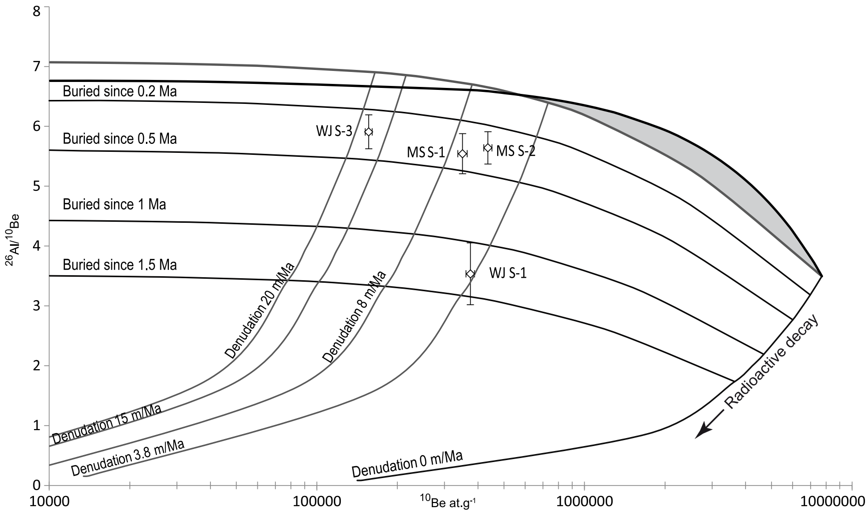

Fig. 5. Evolution of the $^{26}Al/^{10}Be$ ratio as a function of the ^{10}Be concentrations for the four quartz pebbles from Mansu-Ri (Loc. IV) and Wondang-Jangnamgyo, South Korea. The upper bold curve corresponds to surface rocks exposed to cosmic radiation during finite time periods and experiencing no denudation while the lower bold curve corresponds to surface rocks exposed to cosmic radiation during an infinite time period and experiencing finite denudation rates. For both curves, both neutrons and muons induced productions were accounted for in the total production. The grey zone is the "island of the stationary states". It includes all results corresponding to surface samples having undergone a simple exposure history to cosmic rays at the top of surfaces affected by different denudation rates. Above and on the right side of the curves lies "the forbidden area" where the results cannot be geologically interpreted. The white zone beneath the bold curves corresponds to the "burial area" where the results can only be interpreted invoking a burial episode. The thin black curves characterize burial duration of 0.5 and 1 Ma, as indicated. The thin grey curves correspond to different denudation rates. The diamonds highlight the four studied pebbles. The vertical bars associated to the diamonds represent the ^{10}Be concentration uncertainties ($\pm 1\sigma$) and the horizontal ones the $^{26}Al/^{10}Be$ ratio uncertainties ($\pm 1\sigma$). MS S-1 = MS^{10}BeS-1; MS S-2 = MS^{10}BeS-2; WJ S-1 = WJ^{10}BeS.1; WJ S-3 = WJ^{10}BeS.3.

Fig. 5. Évolution du rapport $^{26}Al/^{10}Be$ en fonction des concentrations en ^{10}Be pour les quatre galets de quartz venant de Mansu-Ri (Loc. IV) et Wondang-Jangnamgyo, Corée du Sud. La courbe épaisse supérieure correspond aux roches de surface exposées au rayonnement cosmique pendant des périodes de temps finies dans des conditions d'érosion nulle et la courbe épaisse inférieure correspond aux roches de surface exposées au rayonnement cosmique pendant une période de temps infinie, mais pour des taux de dénudation finis. Pour ces deux courbes, les productions de neutrons et de muons ont été prises en compte dans la production totale. La zone grise est « l'îlot des états stationnaires ». Il comprend tous les résultats correspondant à des échantillons de surface ayant été soumis à une histoire unique d'exposition au rayonnement cosmique au sommet de surfaces affectées par différents taux de dénudation. La zone blanche sous les courbes épaisses correspond à la zone d'enfouissement où les résultats peuvent uniquement être interprétés en évoquant un épisode d'enfouissement. Les fines courbes noires caractérisent des durées d'enfouissement de 0,5 et 1 Ma, comme indiqué. Les fines courbes grises correspondent à différents taux de dénudation. Si les valeurs sont reportées en dehors des zones blanche et grise, les résultats ne peuvent être géologiquement interprétés. Les losanges représentent les résultats obtenus pour les quatre galets étudiés. Les barres verticales associées aux losanges représentent les incertitudes des concentrations en ^{10}Be ($\pm 1\sigma$) et les barres horizontales les incertitudes sur le rapport $^{26}Al/^{10}Be$ ($\pm 1\sigma$). MS S-1 = MS^{10}BeS-1 ; MS S-2 = MS^{10}BeS-2 ; WJ S-1 = WJ^{10}BeS-1 ; WJ S-3 = WJ^{10}BeS-3.

Jangnamgyo (c and d, Fig. 4) sampled ~2 m beneath the surface are presented in Table 1. In Fig. 5, they are plotted on a graph (exposure–burial diagram; e.g., Granger, 2006) presenting the evolution of the $^{26}Al/^{10}Be$ ratio as a function of the ^{10}Be concentration.

Regarding the four studied quartz pebbles, the minimum burial durations obtained with the model without post-burial production range from 331.9 ± 18.0 ka to 1.28 ± 0.19 Ma associated with denudation rates between 3.9 ± 0.6 m Ma^{-1} to 17.8 ± 0.9 m Ma^{-1}. In the exposure–burial diagram (Fig. 5), the pebbles all located in the "burial area" lead to minimum burial durations ranging from 325 ± 100 ka for the youngest (WJ^{10}BeS-3) and to 1.28 ± 0.30 Ma for the oldest (WJ^{10}BeS-1) and denudation rates affecting the overlying surfaces ranging from 4.0 to 17.7 m.Ma^{-1}, similar to the data obtained performing the model without post-burial production. However, it is worth mentioning that in both sites the samples were not deeply buried, especially those from Wondang-Jangnamgyo and that therefore, due to the thin soil cover, post production may have occurred leading to burial durations that should be longer. Performing the model with post-burial production to thus consider possible cosmogenic nuclide production during burial yields maximized burial durations and denudation rates ranging from 382.4 ± 20.8 ka to 2.77 ± 0.41 Ma and from 2.5 ± 0.4 m Ma^{-1} to 18.8 ± 0.9 m Ma^{-1}, respectively. The denudation rate ranges obtained by the three methods are similar and the rates at the Mansu-Ri (Loc. IV) site are consistent.

Due to the sampling depths, the post-burial cosmogenic nuclide production is significant at both sites, between 3 and 7% at the Mansu-ri (Loc. IV) site and 16 to 67% at the Wondang-Jangnamgyo site.

Due to the data dispersion, no weighted mean burial duration can be calculated. Considering the individual durations and their associated uncertainties at the Mansu-Ri (Loc. IV) site, the burial duration of the two quartz pebbles from the archaeological level 5-c is longer than 235 ka (obtained by subtracting it uncertainty to the youngest age [MS^{10}Be S-2] derived from the diagram, that is 330–95 = 235 ka), but shorter than 494.6 ka (obtained by adding it uncertainty to the oldest age [MS^{10}Be S-1] derived from the model with post-burial production,

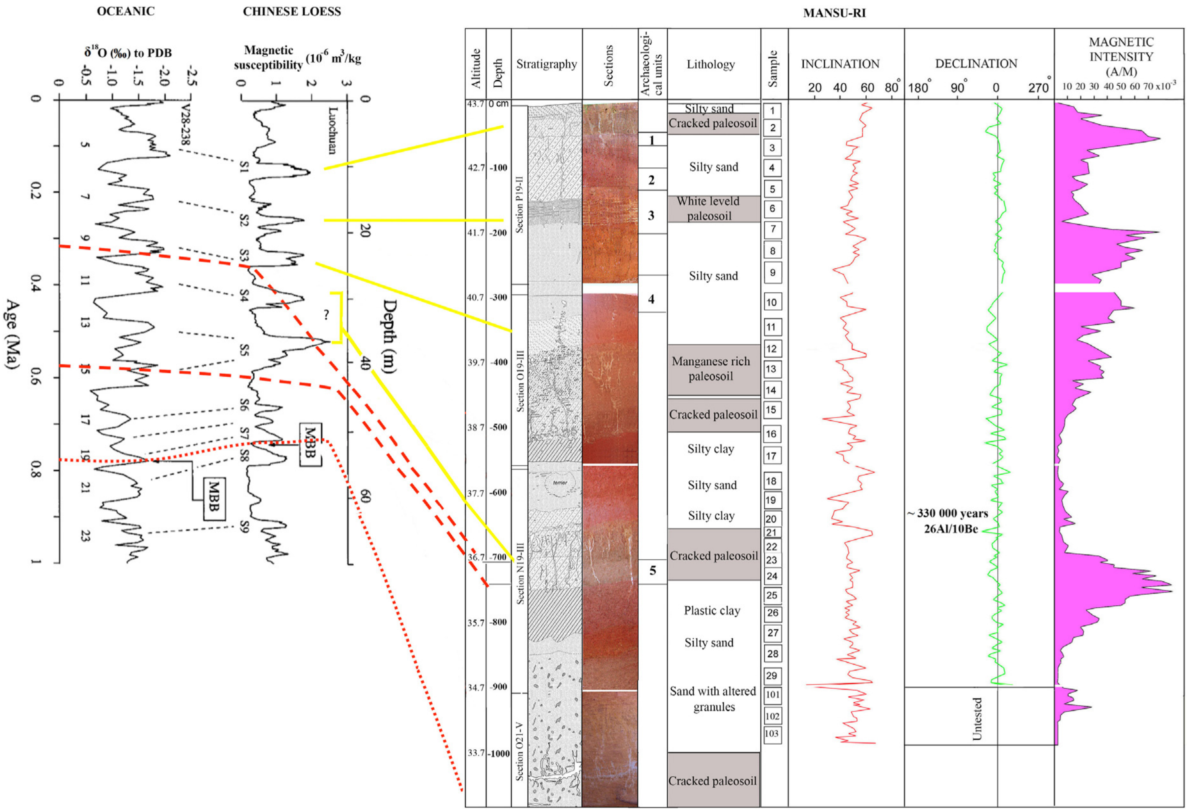

Fig. 6. Mansu-Ri, Locality IV. Stratigraphy and paleomagnetic measurements (inclination, declination and magnetic intensity) in correlation with the Chinese loess magnetic susceptibility and oceanic oxygen isotopic curve (Zhou and Shackleton, 1999). The natural magnetization intensity and the position of the paleosoils is presented for Mansu-Ri. The ages indicated for the Mansu-Ri archaeological unit 5 correspond to the minimum and maximum burial duration averages of the two pebbles (red bold dashed lines). The thin red dashed lines indicate age within the Brunhes period (< 780 ka) all along the sequence. MBB: Matuyama–Brunhes Boundary.

Fig. 6. Mansu-Ri, localité IV. Stratigraphie et mesures paléomagnétiques (inclinaison, déclinaison et intensité magnétique) en corrélation avec les courbes de susceptibilité magnétique des lœss chinois et des isotopes de l'oxygène dans l'océan (Zhou et Shackleton, 1999). L'intensité de magnétisation naturelle et la position des paléosols sont représentées pour Mansu-Ri. Les âges indiqués pour le niveau archéologique 5 de Mansu-Ri correspondent aux moyennes des durées minimum et maximum d'enfouissement des deux galets (tirets rouges épais). Les lignes rouges fines en pointillé indiquent un âge compris dans la période de Brunhes (< 780 ka) pour toute la séquence. MBB : Matuyama–Brunhes Boundary.

that is 464.2 + 30.4 = 494.6 ka). Similarly, at the Wondang-Jangnamgyo site, the burial duration of the WJ^{10}Be S-3 quartz pebble coming from the archaeological level V is longer than 225 ka, but shorter than 621.2 ka.

4.2. Preliminary Magnetic results on the Mansu-Ri site

The raw NRM intensity values of the sediment range between 30 and 80 × 10^{-3} A/m (Fig. 6). The maximum values occur in the sandy silt and in the plastic silty clay, at the base of the paleosoils (50 à 80 × 10^{-3} A/m). The minimum values occur in paleosoils and sandy levels (< 10 × 10^{-3} A/m). The high magnetic intensity values below the paleosoils may result from an intense weathering of the sediments followed by a downward migration of the iron oxides which then accumulated in the underlying sedimentary layers. These accumulations of iron oxide suggest that the deposits underwent, at least, four hot and wet climatic periods.

When confronted with the Chinese loess record, the high NRM intensity values measured along the sedimentary deposit section at Mansu-Ri (Locality IV) correspond to the high magnetic susceptibility values measured along the S1 to S5 Chinese soils (Fig. 6).

The inclination of the magnetic components varies between 34° and 66°. Nevertheless, the base of core 29 presents a significantly lower value of 14°. The declination of cores 1 to 29 exhibits values close to 0°.

Generally, all the cores analyzed in this locality present a normal magnetic polarity, similar to the current polarity. The average inclination is of the order of 50°, similar to the current inclination measured at Chengwon (South Korea) equals to 52°.

This normal polarity sequence can be thus undoubtedly awarded to the period of Brunhes younger than 780,000 years, with no hints of an excursional record.

5. Discussion-conclusion

Three of the samples from the two Early Paleolithic studied sites located more than 150 km away show similar burial durations. The similarity of the ^{26}Al/^{10}Be ratio of the two Mansu-Ri artifacts sampled at the same depth strongly suggests that they likely have the same exposure-burial history. However, sample MS^{10}BeS-2 presents higher ^{10}Be and ^{26}Al concentrations than sample MS^{10}BeS-1, suggesting that they may initially have been within the same deposit but with sample MS^{10}BeS-2 being above MS^{10}BeS-1. The simplest explanation of the burial duration difference between the two pebbles from Wondang-Jangnamgyo is that the oldest sample (WJ^{10}BeS-1) has a complex history of successive burials and expositions during which the pebble may have spent some time buried in another sedimentary section before to be reworked and rapidly re-sedimented in the Wondang-Jangnamgyo section. In such a scenario, the last burial event starts with an initial ^{26}Al/^{10}Be ratio significantly lower than 6.61.

This study represents the first burial duration estimations of the archeological layers at the Mansu-Ri (Loc. IV) and Wondang-Jangnamgyo areas and provides the first chronological framework for Early Paleolithic sites in South Korea. At Wondang-Jangnamgyo and Mansu-Ri (Loc. IV), the determined burial durations ranging from ∼225 ka to ∼621 ka and ∼235 ka to ∼495 ka connect the lithic industries found in the V and 5-c archaeological units, respectively, to the end of the time period covering the early Paleolithic.

Interestingly, by analogy with the Chinese loess section, the obtained minimum burial durations are coherent with the interpretation associating to glacial cycles the 3 paleosoils covering the samples dated at Mansu-Ri. Using the presented preliminary results, a correlation based on magnetic susceptibility curves is thus proposed between the Chinese loess and the Mansu-Ri section (Fig. 6). These two studied sites are, according to the results, at least 200 ka younger than the Chinese Bose and Zoukoudian Acheulean site (Guanjun Shen et al., 2009; Wang et al., 2006).

Constraining burial durations of the selected archaeological layers will necessitate undergoing determination of the deposition rates of the shallow sedimentary layers overlying the layers of interest.

Acknowledgments

This research was supported by the French Ministry for Foreign Affairs through the French-Korean programs (PHC STAR) on the ancient Paleolithic of Korea (n° 21469YC). The authors thank L. Leanni, M. Arnold, G. Aumaître and K. Keddadouche for their respective valuable assistance during chemical treatments, ICP-OES measurements and ^{10}Be and ^{26}Al measurements at the ASTER AMS national facility (CEREGE, Aix-en-Provence) which is supported by the INSU/CNRS, the ANR through the “Projets thématiques d’excellence” program for the “Equipements d’excellence” ASTER-CEREGE action, IRD and CEA. Thanks also to Ph. Dussoulliez for artwork support. Professor Henry de Lumley is gratefully acknowledged for the opportunity given to work on such archaeological sites.

References

Bourlès, D.L., 1992. Beryllium isotopes in the Earth’s Environment. Encyclopedia of Earth System Science, Vol. 1. Academic Press, pp. 337–352.

Braucher, R., Merchel, S., Borgomano, J., Bourlès, D.L., 2011. Production of cosmogenic radionuclides at great depth: A multi element approach. Earth Planet. Sci. Lett. 309 (1), 1–9.

Chmeleff, J., von Blanckenburg, F., Kossert, K., Jackob, D., 2010. Determination of the ^{10}Be half-life by multicollector ICP-MS and liquid scintillation counting. Nucl. Inst. Meth. B 268 (2), 192–199.

Carbonell, E., Bermudez de Castro, J.M., Parés, J.M., Pérez-Gonzalez, A., Cuenca-Bescos, G., Ollé, M., Mosquera, A., Huguet, R., van der Made, J., Rosas, A., Sala, R., Vallverdu, J., Garcia, N., Granger, D.E., Martinon-Torres, M., Rodriguez, X.P., Stock, G.M., Vergès, J.M., Allué, E., Burjachs, F., Caceres, I., Canals, A., Benito, A., Diez, C., Lozano, M., Mateos, A., Navazo, M., Rodriguez, J., Rosell, J., Arsuaga, J.L., 2008. The first hominin of Europe. Nature 452, 465–469.

Gibbon, R.J., Granger, D.E., Kuman, K., Partridge, T.C., 2009. Early Acheulean technology in the Rietputs Formation, South Africa, dated with cosmogenic nuclides. J. Hum. Evol. 56, 152–160.

Granger, D.E., 2006. A review of burial dating methods using ^{26}Al and ^{10}Be. In: Siame, L.L., Bourlès, D., Brown, E.T. (Eds.), Geological Society of America, Special paper, 415, pp. 1–16.

Granger, D.E., Muzikar, P.F., 2001. Dating sediment burial with in situ-produced cosmogenic nuclides: theory, techniques, and limitations. Earth Planet. Sci. Lett. 188, 269–281.

Granger, D.E., Gibbon, R.J., Kuman, K., Clarke, R.J., Bruxelles, L., Caffee, M.W., 2015. New cosmogenic burial ages for Sterkfontein Member 2 *Australopithecus* and Member 5 Oldowan. Nature 522, 85–88.

Guanjun Shen, Xing Gao, Bin Gao, Granger, D.E., 2009. Age of Zhoukoudian *Homo erectus* determined with ^{26}Al/^{10}Be burial dating. Nature 458, 198–200.

Korschinek, G., Bergmaier, A., Faestermann, T., Gerstmann, U.C., Knie, K., Rugel, G., Wallner, A., Dillmann, I., Dollinger, G., Lierse von Gosstomski, Ch., Kossert, K., Maiti, M., Poutivtsev, M., Remmert, A., 2010. A new value for the ^{10}Be half-life by Heavy-Ion Elastic Recoil detection and liquid scintillation counting. Nucl. Inst. Meth. B 268 (2), 187–191.

Lebatard, A.-É., Alçiçek, M.C., Rochette, P., Khatib, S., Vialet, A., Boulbes, N., Bourlès, D.L., Demory, F., Guipert, G., Mayda, S., Titov, V.V., Vidal, L., Lumley, H. de, 2014a. Dating the *Homo erectus* bearing travertine from Kocabas, (Denizli, Turkey) at least 1.1 Ma. Earth Planet. Sci. Lett. 390, 8–18.

Lebatard, A.-É., Bourlès, D.L., Alçiçek, M.C., 2014b. Datation des travertins de Kocabaş par la méthode des nucléides cosmogéniques ^{26}Al/^{10}Be. L’Anthropologie 118 (1), 34–43.

Lumley, H. de, Cauche, D., Celiberti, V., Khatib, S., Lartigot-Campin, A.-S., Lebatard, A.-E., Lebegue, F., Menras, C., Mestour, B., Moigne, A.-M., Moles, V., Moulle, P.-E., Notter, O., Perrenoud, C., Rochette, P., Rossoni, E., Saos, T., Vialet, A., Wengler, L., Bourles, D., Braucher, R., Lee, Y.-J., Park, Y.-C., Han, C.-G., Bae, K., Yi, S., Hong, M.-Y., Cho, T.-S., Kong, S., Choi, M.-C., Choi, S.-Y., Jung, S.-E., 2011. Les industries du Paléolithique ancien de Corée du Sud dans leur contexte stratigraphique et paléoécologique. Leur place parmi les cultures du Paléolithique ancien en Eurasie et en Afrique. CNRS Editions, Paris, 631 p.

Molliex, S., Siame, L.L., Bourlès, D.L., Bellier, O., Braucher, R., Clauzon, G., 2013. Quaternary evolution of a large alluvial fan in a periglacial setting (Crau Plain, SE France) constrained by terrestrial cosmogenic nuclide (^{10}Be). Geomorphology 195, 45–52.

Pappu, S., Gunell, Y., Akhilesh, K., Braucher, R., Taieb, M., Demory, F., Thouveny, N., 2011. Early Pleistocene presence of Acheulian hominins in South India. Science 331, 1596–1599.

Samworth, E.A., Warburton, E.K., Engelbertink, G.A.P., 1972. Beta decay of the ^{26}Al ground state. Phys. Rev. C5, 138–142.

Stone, J.O., 2000. Air pressure and cosmogenic isotope production. J. Geophys. Res. 105 (B10), 23753–23759.

Wang, W., Mo, J.Y., Huang, Z.T., 2006. Recent discovery of handaxes associated with tektites in the Nanbanshan locality of the Damei site, Bose Basin, Guangxi, South China. Chin. Sci. Bull. 51, 2161–2165 (in Chinese).

Zhou, L.P., Shackleton, N.J., 1999. Misleading positions of geomagnetic reversal boundaries in Eurasian loess and implications for correlation between continental and marine sedimentary sequences. Earth Planet. Sci. Lett. 168, 117–130.